IL NUOVO CIMENTO **44 C** (2021) 19
DOI 10.1393/ncc/i2021-21019-4

COMMUNICATIONS: SIF Congress 2020

^{6}Li-enriched LiF films grown by thermal evaporation for neutron detection

V. NIGRO([1]) on behalf of R. M. MONTEREALI([1]), E. NICHELATTI([2]), A. RUFOLONI([1]) and M. A. VINCENTI([1])

([1]) *ENEA R.C. Frascati, Fusion and Technologies for Nuclear Safety and Security Dept. Via E. Fermi, 45, 00044 Frascati, Rome, Italy*
([2]) *ENEA R.C. Casaccia, Fusion and Technologies for Nuclear Safety and Security Dept. Via Anguillarese, 301, 00123 S. Maria di Galeria, Rome, Italy*

received 11 February 2021

Summary. — The new generation of neutron detectors based on ^{6}LiF thin films has been widely investigated in the last decades. The structure of polycristalline thin films has a significant impact upon their performance in neutron detectors, however the relationship between the physical properties of LiF-based thin films and their performance is still far from being completely understood. A systematic investigation of the role played by the growth conditions on the optical and morphological properties of thermally evaporated ^{6}LiF thin films has been carried out by combining spectrophotometry, stylus profilometry and atomic force microscopy. A clear picture of the influence of film thickness and deposition temperature on transparency, porosity, roughness and grain size of polycristalline ^{6}LiF thin films thermally evaporated on amorphous substrates has been obtained.

1. – Introduction

Interest on neutrons for their application in radiation therapies for cancer treatment, in radioprotection and nuclear decommissioning or as useful probe for investigating condensed matter has hugely increased in the last 20 years. Neutron detection is a primary issue when dealing with nuclear reactors, either fusion or fission ones. However, the increasing demand of ^{3}He, a common component in neutron detectors, has caused its shortage with a very large cost increase, which is currently weakening scientific research and nuclear safety. This situation has motivated the scientific community to develop a new generation of neutron detectors to replace the ^{3}He-based systems. Novel materials have been therefore investigated as neutron converters into charged particles that emerge with sufficiently high energy to produce a measurable electrical signal once combined with a charged-particle detector [1-4].

In searching for nuclear reactions that might be useful in neutron detection, several factors must be considered. The cross-section of the reaction must be as large as possible so that efficient detectors can be built with small dimensions. For the same reason the target nuclide should be of high isotopic abundance in the natural element, or alternatively, should be an economic source of artificially enriched samples available for detector fabrication. In many applications, intense fields of gamma rays are also found with neutrons and the choice of reaction bears on the ability to discriminate against these gamma rays in the detection process. Moreover, their application in neutron reactors requires high resistance to very harsh environments (high temperature, high pressure, high neutron fluxes, etc.). The ideal neutron detector should be therefore compact, fissile-material-free, radiation- and temperature-resistant and, last but not least, it should be sensitive to both thermal and fast neutrons.

Traditionally neutron detectors involve the combination of a target material designed to carry out the nuclear conversion together with one conventional radiation detector. One of the most promising materials for detection of neutrons is lithium fluoride (LiF), as one of lithium isotopes, ^{6}Li, has a very high cross-section for (n, α) reaction with thermal neutrons and it rapidly decreases with increasing neutron energy [5]. Natural lithium contains indeed about 7.5% of ^{6}Li isotope and 92.5% of ^{7}Li isotope, making it possible to convert neutrons to directly detectable charged particles through the nuclear reaction $^6\mathrm{Li}(n, \alpha)^3\mathrm{H}$:

$$^6\mathrm{Li} + n \longrightarrow {}^3\mathrm{H} + {}^4\mathrm{He} + 4.79 \text{ MeV}, \tag{1}$$

with tritium ions and α-particles emitted in opposite directions with energies 2.73 and 2.07 MeV, respectively.

Therefore many types of charged-particle detector techniques, such as gas counters, ionization chambers, scintillation detectors and semiconductor detectors can be used, while sensitivity to thermal neutrons can be achieved by depositing a lithium-6 fluoride (^{6}LiF) layer on top of the conventional detector [6-8].

In the last ten years many attempts have been made to develop solid-state neutron detectors based on chemical vapour deposition (CVD) single-crystal diamond or silicon detectors functionalized with ^{6}LiF films for application in neutron reactors with high neutron fluxes [9-11]. Compact solid-state neutron detectors capable of simultaneously detecting thermal and fast neutrons have been succesfully tested in collaboration with the ENEA Frascati Research Centre [6,12,13]. The detectors have been fabricated from CVD single-crystal diamond films covered with a 95% enriched ^{6}LiF film deposited on top of the upper metal contact by thermal evaporation in a dedicated evaporation facility [14] at the FSN-TECFIS-MNF Laboratory at ENEA Frascati Research Centre. Fast neutrons are directly detected in the CVD diamond bulk, since they have enough energy to produce the $^{12}\mathrm{C}(n, \alpha)^9\mathrm{Be}$ reaction in diamond. Thermal neutrons are instead converted into charged particles in the ^{6}LiF layer through the $^6\mathrm{Li}(n, \alpha)^3\mathrm{H}$ nuclear reaction and then detected in the diamond layer. The analysis of the nuclear reaction kinematics has allowed to calculate the resolution and sensitivity of the detector for both fast and thermal neutrons. It has been shown that the detection process of thermal neutrons is highly influenced by the ^{6}LiF layer thickness: the thicker the ^{6}LiF layer, the higher the conversion efficiency and the counting rate. On the other hand, tritium ions and α-particles lose part of their energy in the ^{6}LiF layer, so that optimal energy resolution calls for thin layers [6]. It is therefore crucial finding the film thickness for the best trade-off between conversion efficiency, counting rate and energy resolution for their standard use with neutrons.

Besides detection of directly ionizing particles in electrically driven radiation detectors, Fluorescent Nuclear Track Detectors (FNTD) mainly based on sapphire (Al_2O_3) materials, have also been effectively applied for measurements of low neutron doses. Developed during the last decade by Akselrod and coworkers [15], their operation is based on radiophotoluminescence (RPL), *i.e.*, photoluminescence of radiation-induced electronic defects. Another material exhibiting this phenomenon is LiF. Many kinds of radiations create F centres in LiF, *i.e.*, anion vacancies with trapped electron, which in turn tend to aggregate into more complex defects. RPL of LiF is related to the stable F_2 and F_3^+ centres, F_2 consisting of two anion vacancies with two bound electrons and F_3^+ of three anion vacancies with two bound electrons. Both these centres may be excited with blue light and upon return to the ground state, luminescence is emitted with a broad spectrum consisting of two bands, one peaked at 678 nm (related to F_2), and one peaked at 541 nm (related to F_3^+) [16].

Very recently Bilski and coworkers investigated natural LiF crystals for fluorescent detection of nuclear tracks [17, 18]. They showed that visible RPL signal of radiation-induced colour-centres in LiF crystals is high enough to visualize tracks of a single charged particle by using wide-field fluorescence microscopy. Indeed, in fluorescent tracks registered after irradiation with thermal neutrons two different opposite features have been distinguished: one shorter (6 μm) and brighter and one longer (33 μm), whose lengths well agree with the predicted ranges in LiF of the alpha particle and the tritium nucleus produced by the $^6\mathrm{Li}(n,\alpha)^3\mathrm{H}$ nuclear reaction. Further improvements on the sensitivity of LiF-based FNTDs may be achieved by growing LiF crystals from ^{6}Li-enriched lithium, with an expected enhancement of the number of registered tracks by a factor 10 and an increase of the detector efficiency allowing their use in individual dosimetry [19, 20]. On the other hand, the possibility to develop neutron detectors based on thin layers may allow to reduce the gamma background observed in FNTDs based on LiF crystals.

In this framework the structure of polycristalline thin films has significant influence upon their performance and a good control of the optical and morphological properties of ^{6}LiF thin films is crucial to improve the efficiency of LiF-based neutron detectors. Nevertheless the relationship between the physical properties of ^{6}LiF thin films and the performance of ^{6}LiF-based detectors is still far from being completely understood. In this regard the systematic investigation of the role played by growth conditions on the physical properties of ^{6}LiF thin films, such as transparency, porosity, roughness and grain size, will open the way to further improvements in these novel neutron detection techniques.

2. – Materials and methods

Polycrystalline thin films of 95%-enriched ^{6}LiF were grown by thermal evaporation on glass substrates at the ENEA Frascati Research Centre through the GP20 deposition system of SISTEC-Angeloni S.p.A., under controlled experimental conditions [14]. The deposition process was performed in a vacuum chamber at a pressure lower than 10^{-3} Pa, keeping the substrate temperature (T_s) constant at 35 °C, 100 °C and 300 °C in each deposition run. The starting material, consisting of commercially available 95%-enriched ^{6}LiF pellets, was heated at about 850 °C in a water-cooled tantalum crucible, placed below the substrate holder at a distance of 22 cm. The nominal film thickness (t_{nom}) and the evaporation rate were monitored *in situ* by an INFICON quartz oscillator. The same experimental conditions were used for thermal deposition of 95%-enriched ^{6}LiF films on diamond detectors under test at the Frascati Neutron Generator [21] and at the Joint European Torus [9, 12, 13].

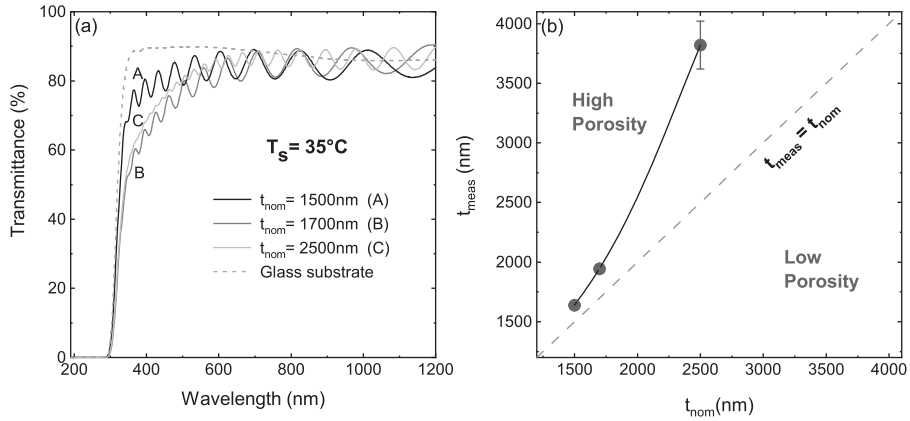

Fig. 1. – (a) Transmittance of ^{6}LiF thin films of nominal thickness 1500 nm, 1700 nm and 2500 nm grown by thermal evaporation on glass substrates at T_s = 35 °C. The dashed line is the transmittance of the bare glass substrate. (b) Behaviour of the measured thickness by profilometry as a function of the nominal thickness as provided by the *in situ* quartz oscillator for ^{6}LiF thin films grown on glass substrate at T_s = 35 °C. The solid line is a guide for eyes. The dashed line with unitary slope is the ideal relationship between the measured and the nominal thicknesses.

The optical properties of ^{6}LiF thin films were investigated by UV-VIS-NIR spectrophotometer (Perkin Elmer Lambda 950) in the wavelength range λ = (190–1200) nm at the FSN-TECFIS-MNF Laboratory of ENEA Frascati. The thickness of the deposited ^{6}LiF films was measured after the growth by using a stylus profilometer (KLA-Tencor, P-1 model) at the DTE-FSD-TEF Laboratory of ENEA Casaccia. In the following, it is referred to as "measured thickness" (t_{meas}). The morphological characterization of ^{6}LiF thin films was performed by a PARK System Atomic Force Microscopy (AFM), model XE-150 operating in air in non-contact mode, at the FSN-COND Laboratory of ENEA Frascati.

3. – Results and discussion

Optical, structural and morphological properties of ^{6}LiF films grown on amorphous substrates, such as glass, strongly depend on the deposition parameters. Figure 1(a) shows the transmission spectra of ^{6}LiF thin films of nominal thickness 1500 nm, 1700 nm and 2500 nm grown on glass substrates at T_s = 35 °C together with the transmittance of the bare substrate. These spectra show that the thermally evaporated ^{6}LiF films are characterized by high optical transmission: for wavelengths higher than 600 nm, optical transmission is greater than 80% regardless of the film nominal thickness; at shorter wavelengths, between 300 nm and 500 nm, the 1500 nm thick film exhibits the highest optical transmission, indicating the highest optical transparency in the UV range for the thinnest film. The typical interference pattern, due to the difference of the refractive index between ^{6}LiF film and glass substrate, is a signature of the film good optical quality, planarity and uniformity. In fig. 1(b) the behaviour of the measured thickness (t_{meas}) as a function of the nominal thickness (t_{nom}), for ^{6}LiF thin films grown by thermal evaporation on glass substrate at T_s = 35 °C, is reported. At this substrate temperature, the measured thickness is higher than the nominal one, probably due to

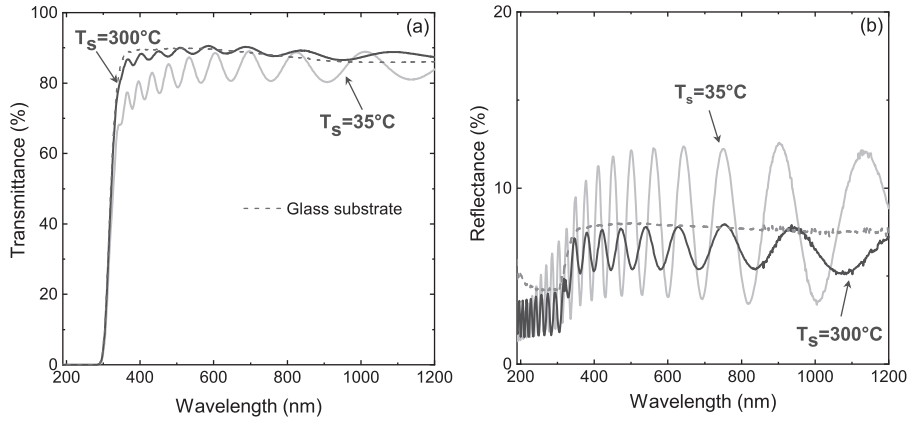

Fig. 2. – (a) Transmittance and (b) reflectance spectra for ^{6}LiF thin films of 1500 nm nominal thickness grown on glass substrates at $T_s = 35$ °C and $T_s = 300$ °C by thermal evaporation. Dashed lines are transmittance and reflectance spectra for the bare glass substrate.

the inner porosity of the film, becoming more and more porous as the thickness increases. As a result of the deposition conditions and of the substrate surface structure, LiF thin films grown on amorphous substrates are indeed polycrystalline [22], consisting of many single monocrystals known as grains. The film can be therefore considered as an aggregate of material grains separated by air interstices that reduce the layer density.

Adjusting the film thickness is therefore an important part of tuning the film density and its optical transparency. However a crucial role is also played by the deposition temperature. To investigate its influence on the optical properties of thin films, ^{6}LiF films were thermally evaporated on glass substrates at different temperatures in the range $T_s = (35–300)$ °C. In fig. 2(a) the transmittance spectra of ^{6}LiF films of $t_{nom} = 1500$ nm grown at $T_s = 300$ °C and $T_s = 35$ °C are reported together with the transmittance of the bare glass substrate. At $T_s = 300$ °C the highest transmittance values ($\approx 90\%$) are obtained in the whole investigated wavelength range. Below $\lambda = 600$ nm the transmittance decreases with decreasing substrate temperature, suggesting an increase of volume scattering, which may be due to porosity. Figure 2(b) shows the reflectance for the same ^{6}LiF films of 1500 nm nominal thickness grown at $T_s = 300$ °C and $T_s = 35$ °C compared with the optical reflectance of the bare glass substrate. The typical interference pattern due to the thin film is plainly evident over the entire wavelength range, with the fringe amplitude decreasing when the substrate temperature increases. The difference between the refractive index of the film and the refractive index of the bare substrate is indeed supposed to decrease with increasing substrate temperature. As a matter of fact, the refractive index is strongly related to the density of the deposited film, which is in turn dependent on the film structure.

According to ref. [23], higher substrate temperatures increase the mobility of the film molecules and thus favour the formation of more tightly packed microcrystals. As a consequence ^{6}LiF thin films grown at $T_s = 300$ °C are expected to be more homogeneous and less porous. A possible way to monitor the behaviour of the porosity is through the ratio between the measured and the nominal thickness, the first provided by profilometry and the latter by the *in situ* quartz oscillator. Values of $t_{meas}/t_{nom} > 1$ found at $T_s = 35$ °C and $T_s = 100$ °C, can be attributed to high porosity, while values of

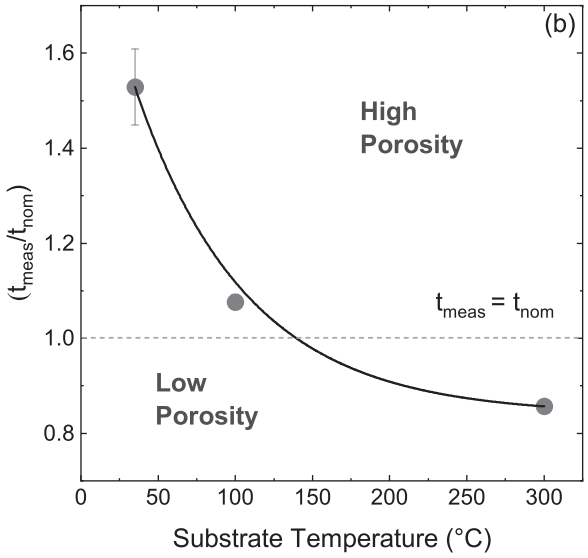

Fig. 3. – Ratio between the thickness of ^{6}LiF films as measured by profilometry and the nominal thickness of the same film as set during the evaporation process as a function of the substrate temperature. The solid line is a guide for eyes. The dashed line with unitary slope is the ideal relationship between the measured and the nominal thicknesses.

$t_{meas}/t_{nom} < 1$ for thin films at $T_s = 300$ °C may indicate the increase of compactness as the substrate temperature increases, resulting in highly packed microstructures and therefore less porous thin films (fig. 3).

This behaviour provides information on the microstructural arrangements of the polycristalline thin films on the amorphous substrate. Their structure has significant influence upon their performance: porosity, grain shape, grain size, grain boundary and grain orientations influencing film properties and stability, highly affect the LiF-based detector efficiency indeed. In particular understanding the relationship between the substrate temperature and the grain growth of the ^{6}LiF thin films is imperative.

Surface morphology of the ^{6}LiF thin films was studied by AFM, as shown in fig. 4 where the 3D and 2D AFM images over an area of (10×10) μm^2 for a ^{6}LiF films ($t_{nom} = 2500$ nm) grown by thermal evaporation at $T_s = 100$ °C are reported as an example. From AFM images we can see that ^{6}LiF films are almost homogeneous and consist of grains of different size, whose features strongly depend on the substrate temperature. In thin films indeed surface roughness may be related to porosity. Both the Root Mean Square (RMS) roughness, defined as the square root of the distribution of surface height, and the average roughness, defined as the mean height as calculated over the entire measured length, were measured along the white lines indicated in fig. 4(b). The interesting decrease of both the RMS and the average roughness with increasing T_s, as shown in fig. 5(a), points out the smoother surface of ^{6}LiF films grown at higher temperature, where smaller grains form (fig. 5(b)). Indeed the average grain size of polycrystalline ^{6}LiF thin films, as estimated from AFM images, is shown to decrease from (160 ± 12) nm at lower temperature to (60 ± 2) nm for higher substrate temperature. These results corroborate the idea that at high temperature the relative stronger influence of migration processes tends to produce a denser and smoother film with less voids, resulting in a lower porosity and smaller roughness [24].

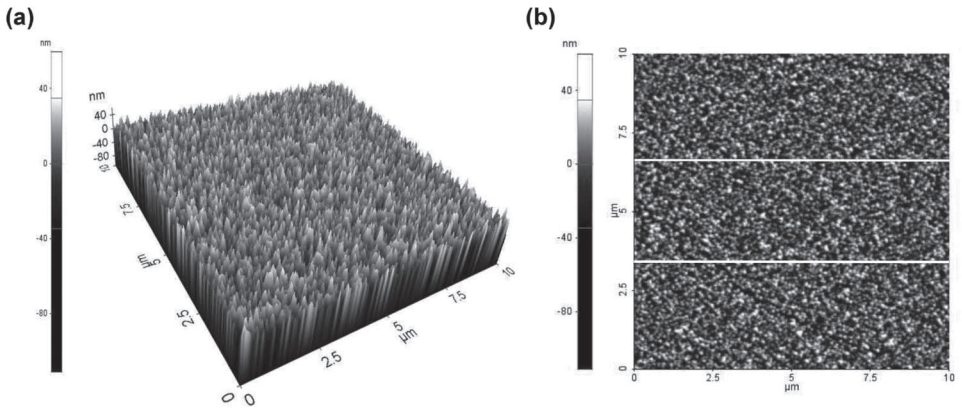

Fig. 4. – (a) 3D and (b) 2D AFM images over an area of (10×10) μm^2 of a ^{6}LiF film, nominal thickness 2500 nm, grown on the glass substrate by thermal evaporation at $T_s = 100$ °C. The white line profiles along which the root mean square roughness was measured are indicated.

4. – Conclusions

Coatings with ^{6}LiF thin films are widely used in conventional neutron detectors for achieving simultaneous detection of thermal and fast neutrons at high doses. More recently, the visible photoluminescence of radiation-induced colour centres in ^{6}LiF can be used in Fluorescent Nuclear Track Detectors with an enhanced sensitivity allowing for their use in neutron dosimetry at very low doses. To achieve a good control of the optical and structural properties of ^{6}LiF thin films and improve their performance in neutron detection, a systematic investigation of the role played by the growth conditions on the physical properties of ^{6}LiF thin films has been reported.

It was observed that for ^{6}LiF thin films thermally evaporated on glass substrates, the higher deposition temperature, the more closely packed configuration is achieved with an

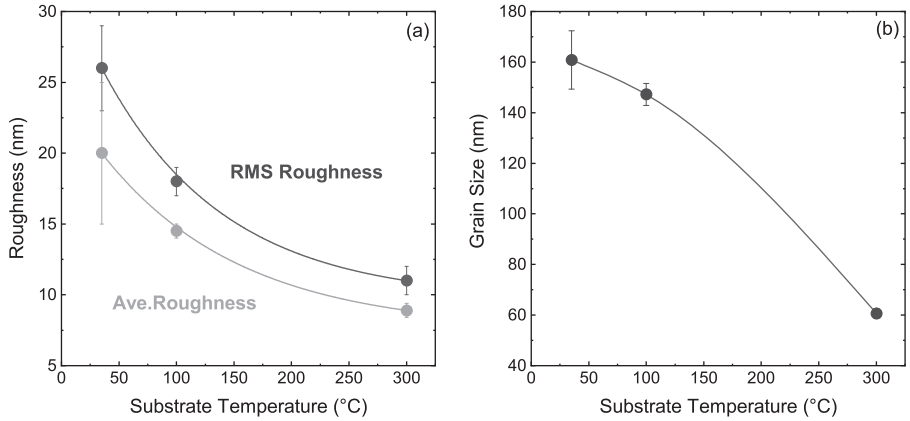

Fig. 5. – (a) RMS roughness and average roughness as functions of the substrate temperature for ^{6}LiF thin films grown on the glass substrates by thermal evaporation. (b) Size of the grains of the polycrystalline ^{6}LiF thin films grown on glass substrates.

expected increase in the film refractive index corresponding to higher optical quality of the thin film. Moreover, as a result of the deposition conditions, ^{6}LiF thin films grown on amorphous substrates are polycrystalline, consisting of many single grains, whose size decreases with increasing deposition temperature. The resulting thin films thermally evaporated at high substrate temperature appear denser and smoother, with low porosity and small roughness. Substrate temperature, besides film thickness, is therefore a good control parameter for transparency, porosity, roughness and grain size of polycristalline ^{6}LiF thin films grown by thermal evaporation on the glass substrate.

* * *

The authors acknowledge Francesca Menchini for the skillful suggestions for profilometry measurements and Mario Tucci of the DTE-FSD-TEF Laboratory of ENEA Casaccia Research Centre for the kind availability. We also thank Maurizio Angelone and Mario Pillon for providing the material and encouraging discussions.

REFERENCES

[1] McGregor D. S. *et al.*, in *2001 IEEE Nuclear Science Symposium Conference Record (Cat. No.01CH37310)*, Vol. **4** (IEEE) 2001, p. 2454.
[2] Bellinger S. *et al.*, *Nucl. Instrum. Methods Phys. Res. Sect. A*, **652** (2011) 387 (*Symposium on Radiation Measurements and Applications (SORMA) XII 2010*).
[3] Finocchiaro P. *et al.*, *EPJ Web of Conferences*, **170** (2018) 01004.
[4] Li Q. *et al.*, *Nucl. Instrum. Methods Phys. Res. Sect. A*, **946** (2019) 162497.
[5] *ENDF/B-VII.1 Library*, `http://www.nndc.bnl.gov/sigma/`.
[6] Almaviva S. *et al.*, *J. Appl. Phys.*, **103** (2008) 054501.
[7] McGregor D. *et al.*, *Nucl. Instrum. Methods Phys. Res. Sect. A*, **608** (2009) 125.
[8] Pappalardo A. *et al.*, *Nucl. Instrum. Methods Phys. Res. Sect. A*, **810** (2016) 6.
[9] Lattanzi D. *et al.*, *Fusion Eng. Des.*, **84** (2009) 1156 (*Proceedings of the 25th Symposium on Fusion Technology*).
[10] Barbagallo M. *et al.*, *Rev. Sci. Instrum.*, **81** (2010) 093503.
[11] Pilotti R. *et al.*, *EPL*, **116** (2016) 42001.
[12] Pillon M. *et al.*, *Fusion Eng. Des.*, **82** (2007) 1174 (*Proceedings of the 24th Symposium on Fusion Technology*).
[13] Angelone M. *et al.*, *Nucl. Instrum. Methods Phys. Res. Sect. A*, **595** (2008) 616.
[14] Vincenti M. *et al.*, Technical Report (Comitato nazionale per la ricerca e per lo sviluppo dell'energia nucleare e delle energie alternative ENEA-RT/DISP) 2013.
[15] Akselrod M. *et al.*, *Radiat. Meas.*, **46** (2011) 1671 (*Proceedings of the 16th Solid State Dosimetry Conference, September 19–24, Sydney, Australia*).
[16] Montereali R. *et al.*, *J. Lumin.*, **170** (2016) 761.
[17] Bilski P. *et al.*, *Radiat. Prot. Dosim.*, **265** (2017) 1.
[18] Bilski P. *et al.*, *Radiat. Meas.*, **116** (2018) 35.
[19] Furuta Y. *et al.*, *Nucl. Instrum. Methods*, **104** (1972) 365.
[20] Sykora G. *et al.*, *Radiat. Meas.*, **43** (2008) 1017 (*Proceedings of the 15th Solid State Dosimetry (SSD15)*).
[21] Marinelli M. *et al.*, *Appl. Phys. Lett.*, **89** (2006) 143509.
[22] Vincenti M. *et al.*, in *Materials Research Proceedings, Part of the book on Photonics and Photoactive Materials*, edited by Prosposito P., Vol. **16** (Materials Research Forum LLC) 2020, pp. 56–64.
[23] Montereali R. M., in *Handbook of Thin Films*, edited by Singh Nalwa H. (Academic Press, Burlington) 2002, Chapt. 7, pp. 399–431.
[24] Hu G. *et al.*, *Phys. Rev. E*, **80** (2009) 041122.